DIELECTRIC, THERMAL AND FUNCTIONAL BEHAVIOR OF BARIUM ZIRCONATE/ EPOXY RESIN NANOCOMPOSITE SYSTEM

Z.-M. Tsikriteas, A. Sanida, S. G. Stavropoulos, A. C. Patsidis and G. C. Psarras

Smart Materials & Nanodielectrics Laboratory, Department of Materials Science,
School of Natural Sciences, University of Patras, Patras 26504, Greece
Email: zmtsikriteas@upnet.gr, ksanida@upatras.gr,
stavropoulos@upatras.gr, patsidis@upatras.gr, G.C.Psarras@upatras.gr,
Web Page: http://smat.lab.upatras.gr

Keywords: Nanocomposites, Nanodielectrics, Barium Zirconate, Smart Materials, Functional Materials, Antiferroelectric Behavior

Abstract

Nanocomposites of epoxy resin and $BaZrO_3$ ceramic nanoparticles were prepared via a mixing process. The electrical response of the epoxy resin/$BaZrO_3$ composite specimens, as well as of barium zirconate nanoparticles was examined by means of broadband dielectric spectroscopy in a wide temperature and frequency range. The real part of dielectric permittivity increases with filler content, although optimum performance does not correspond to the maximum reinforcing phase content. Analysis of the results of dielectric spectroscopy for the nanocomposites revealed the presence of two dielectric relaxations related to the polymeric matrix. The first relaxation is attributed to the transition from the glass to the elastomeric phase of the epoxy resin and is called α-relaxation, while the second one is related to the rearrangement of the lateral polar groups and is called β-relaxation. In addition, the phenomenon of interfacial polarization was observed, due to the presence of inclusions inside the matrix and to the electrical heterogeneity of the composite material. Finally, the ferroelectric and/or anti-ferroelectric behavior of barium zirconate nanoparticles imparts functional performance to the composite system.

1. Introduction

In the last few decades, the development of polymer matrix composite materials reinforced with ceramic inclusions is of particular scientific interest. The combination of these two components leads to dielectrics with optimal behavior. Nanoinclusions add smart material's properties in the composite system through the ability to tailor some of its physical properties, as well as its behavior. In addition, there is a dramatic increase in the interfacial area between the polymer matrix and the filler on account of nanoinclusions' small size (<100 nm). Nanodielectrics are a category of materials engineered for improved performance as dielectrics and electrical insulators. It can be noted that in the dielectrics, the distribution of dipoles and charges can be polarized by an external electric field, so these materials can be used to store electrical energy. Some applications of polymer matrix composites filled with ceramic nanoinclusions are in field of self- current controllers, EMI shielding, conductive adhesives, circuit board welding materials, structural batteries etc [1-5].

Barium Zirconate ($BaZrO_3$) is an important dielectric material that can be used in a variety of applications. Up to now research on Barium Zirconate as a filler is not sufficient, however some of its properties such as high fracture toughness, high melting point (2540°C), high strain resistance etc., make it suitable as reinforcing phase in composites. $BaZrO_3$ has a perovskite structure. In term of barium ziconate's dielectric behavior, it appears to exhibit antiferroelectric behavior [6-7]. The antiferroelectricity theory was proposed by Kittel in 1951 and describe a state in which lines of ions in the crystal are spontaneously polarized, but with neighboring lines polarized in antiparallel directions [8].

2.1. Experimental

In the present study, a set of seven specimens were fabricated by employing commercially available low viscosity epoxy resin (Epoxol 2004 A, Neotex S.A., Athens, Greece), slow rate curing agent (Epoxol 2004 B, Neotex S.A., Athens, Greece) and $BaZrO_3$ nanopowder (<50 nm, Sigma Aldrich). Fabrication of the specimens required initially slow stirring of the resin with the agent, at a weight ratio of 2:1, respectively, for about 5 minutes. Then the $BaZrO_3$ nanoparticles were added by slow precipitation in the mixture and agitating it in the sonicator for another 10 minutes. Later the blends were injected into silicone molds. Finally, the specimens were kept at ambient temperature for 1 week (curing) and then entered an oven at 100 °C for 4 hours (post curing). Filler content is expressed in parts per hundred resin per weight (phr).

Table 1. Features of nanocomposites.

Specimens' content in $BaZrO_3$ (phr)	*Volume Frunction %*	*IP*	α- relaxation	
		E_A (eV)	B (K)	T_V (K)
0 (epoxy)	0	-	18.841	311.686
0.1	0.020	1.364	19.442	311.391
1	0.201	0.883	17.742	311.504
3	0.603	0.687	17.184	308.936
6	1.109	0.700	15.865	308.451
10	1.848	0.479	13.932	310.015
15	2.923	0.684	14.647	306.771

2.1.1. Broadband Dielectric Spectroscopy

The dielectric characterization was conducted by means of broadband dielectric spectroscopy, using an Alpha-N Frequency Response Analyzer and a 1200 BDS dielectric cell, while the temperature control was achieved with the Novotherm system, all provided by Novocontrol.

2.2. Results and Discussion

Plots of the real part of dielectric permittivity (ε') and loss tangent ($tan\delta$) versus frequency and temperature are shown in Fig. 1 and Fig. 2 respectively, for the nanocomposites with 3 and 15 phr barium zirconate content. Note that in this study have been recorded similar spectra for all studied nanocomposites. In Fig. 1 the real part of dielectric permittivity decreases with increasing frequency. It arises from the fact that the dipolar groups can't respond to the high rate of the applied alternating field and so the achieved polarization level of the system diminishes. In contrast, when frequency is low polarization is higher since permanent and included dipoles acquire sufficient time to be aligned parallel to the applied field. In the low frequency region, the effect of temperature is intense resulting in higher ε' values. Three relaxation mechanisms have been detected in the spectra of ε' and $tan\delta$. All specimens demonstrate a process attributed to the transition from the glass to the elastomeric phase of the polymeric matrix, it occurs at intermediate frequencies and is called α-relaxation. At higher frequencies appears β-relaxation due to the rearrangement of polar side groups of the main macromolecular chain. Finally, at low frequencies and high temperatures, another process is observed known as Maxwell- Wagner- Sillars (MWS) effect or Interfacial Polarization (IP). MWS effect is due to the heterogeneity of the composite system.

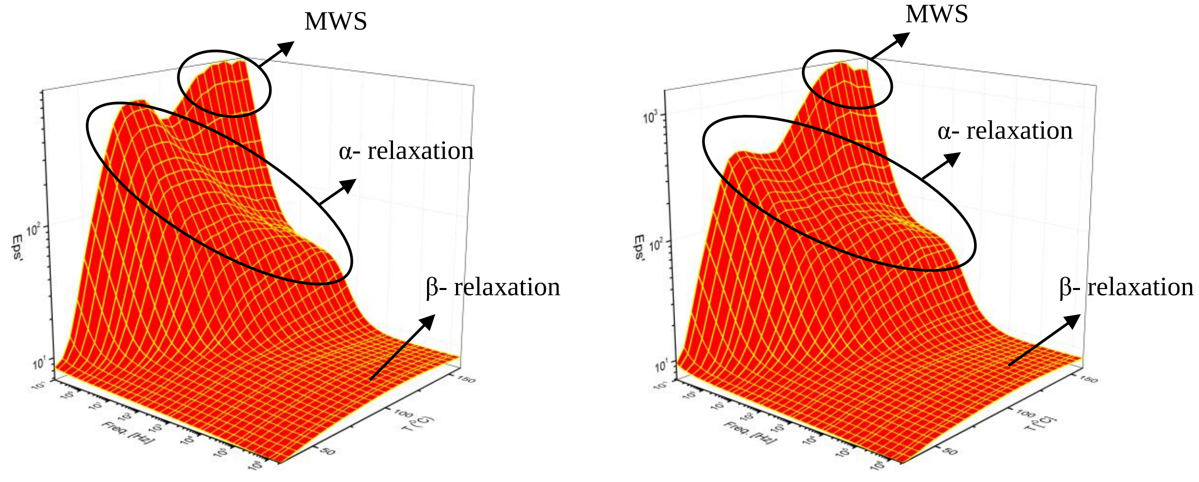

Figure 1. Real part of dielectric permittivity versus frequency and temperature for the nanocomposite with 3 phr $BaZrO_3$ (left) and the nanocomposite with 15 phr $BaZrO_3$ (right).

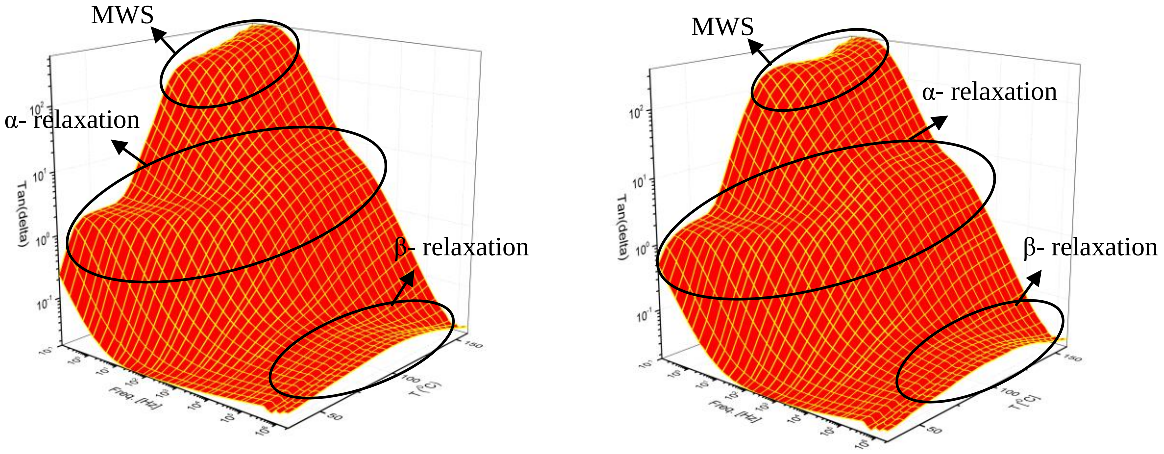

Figure 2. Loss tangent versus frequency and temperature for the nanocomposite with 3 phr $BaZrO_3$ (left) and the nanocomposite with 15 phr $BaZrO_3$ (right).

Fig. 3 shows three dimensional plots of AC conductivity for the nanocomposites with 3 phr and 15 phr $BaZrO_3$ content. AC conductivity is highly dependent on the frequency at low temperatures and its dependence decreases at high temperatures. At constant temperature, dispersion of AC conductivity with frequency can be described via Eq. (1):

$$\sigma_{AC} = \sigma_{DC} + A(\omega)^n \tag{1}$$

where σ_{DC} is the DC value of conductivity and A, n are material’s and temperature depedent parameters. At low frequencies AC conductivity gets or tends to get the constant value of DC conductivity, which increases with the temperature due to higher agility of charges. Nanocomposite appears to be more conductive at higher field frequencies, since charge carriers are able to “hop” between adjacent conductive sites. The 'shoulders' formed are related to the dielectric relaxations of the materials. Finally, higher conductivity is observed in the speciemens with higher content of barium zirconate.

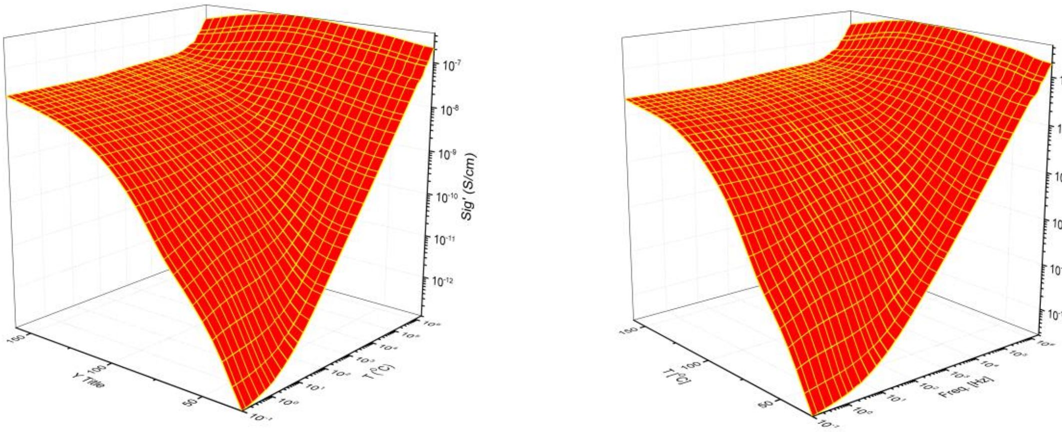

Figure 3. DC conductivity versus frequency and temperature for the nanocomposite with 3 phr $BaZrO_3$ (left) and the nanocomposite with 15 phr $BaZrO_3$ (right).

Fig. 4a presents spectra of the real part of dielectric permittivity versus frequency at various temperatures of barium zirconate. $BaZrO_3$ nanoparticles show an unusual behavior. In common dielectric materials alteration of temperature leads to higher values of permittivity. However, in this case ε' diminishes with the increase of temperature. A similar temperature dependence is shown for AC conductivity in Fig. 4b. Two of the most studied perovskite structures are barium titanate ($BaTiO_3$) and lead zirconate ($PbZrO_3$). Lead zirconate has a Curie temperature at 230°C [9]. Above Curie temperature, $PbZrO_3$ exhibits cubic structure and typical paraelectric behavior. Below $T_{C,}$ crystals of lead zirconate locate in the antiferroelectric state with orthorhombic structure. Near the critical temperature the antiferroelectric phase can take the tetragonal structure of the ferroelectric phase. The mechanism causing this structural differentiation, it's not yet totally clarified. Up to now, it has been attributed to the exert of a strong electrical field or in the presence of impurities [10]. As antiferroelectricity theory, proposed by Kittel in 1951, describes a state in which lines of ions in the crystal are spontaneously polarized, but with neighboring lines polarized in antiparallel directions. The result of such arrangement is a crystal exhibiting macroscopically no spontaneous polarization and thus lower values of ε'. Moreover, as temperature increases further and the ceramic material enters its paraelectric phase the absence of dipolar moments in the unit cells reduces polarization [10-11]. In these cases, a decrease in permittivity' s values as a function of temperature can be observed. Therefore, the unusual behavior of barium zirconate could be an indication for its antiferroelectric character.

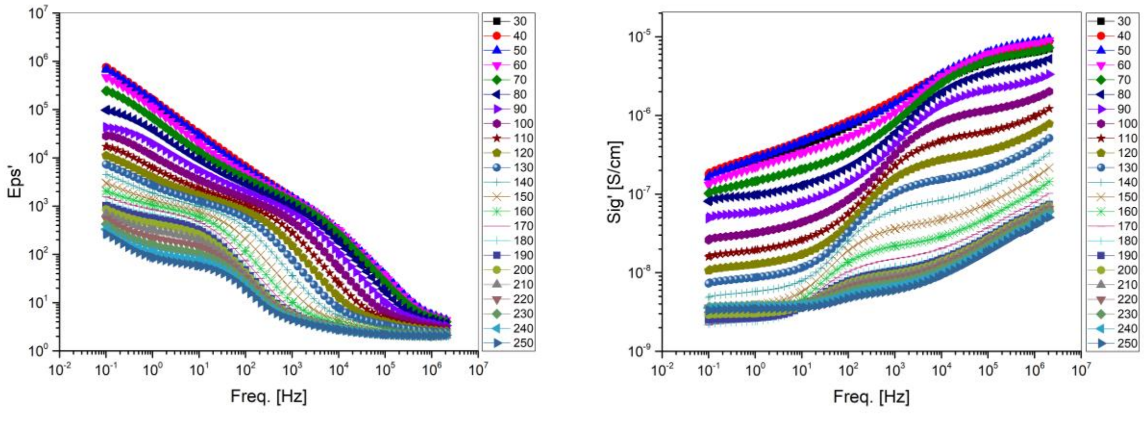

Figure 4. Real part of dielectric permittivity versus frequency for the $BaZrO_3$ nanoparticles (left), and DC conductivity versus frequency for the $BaZrO_3$ nanoparticles (right).

The variation of the real part of dielectric permittivity as a function of frequency, for all the examined systems at 40°C, is represented in Fig. 5a. In all specimens the real part of dielectric permittivity diminishes with frequency and increases with temperature. The reduction of ε' with the frequency is due to the decrease of the achieved polarization as permanent and included dipoles fail to follow the alternation of the applied field, while the augmentation of ε' with temperature is affiliated with the enhanced mobility of macromolecules and dipoles. Furthermore, ε' increases with nanoparticles content. However, the sample with 0.1 phr $BaZrO_3$ content exhibits lower values of permittivity even than the epoxy resin. This behavior has been observed in other ceramic/polymer nanocomposites at low or very low filler content, such as epoxy resin/ $BaSrTiO_3$, epoxy resin/ $SrFe_{12}O_{19}$, epoxy resin/ B_4C and is ascribed to the reduction of polarization because of the exerted obstructions to the mobility of macromolecular dipolar parts [12-13]. In Fig. 5b, in the low-frequency region the phenomenon of interfacial polarization can clearly be observed, caused by the enhanced heterogeneity of the complex system (insulating matrix-semiconductor inclusions).

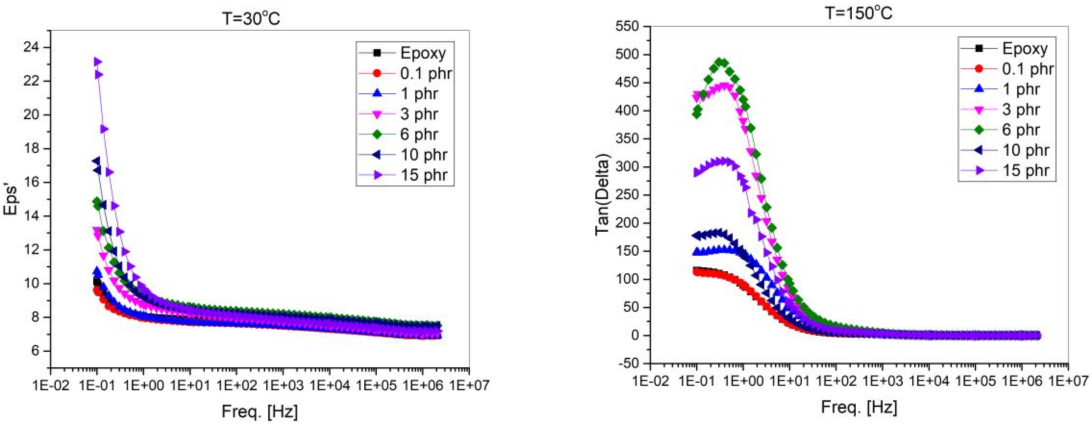

Figure 5. Real part of dielectric permittivity versus frequency at 40 °C for all nanocomposites (left), loss tangent versus frequency at 150 °C for all nanocomposites (right).

Fig. 6a presents the dynamics of the processes or, in other words, the temperature depedance of the loss peak maxima for the interfacial polarization and α-relaxation. IP process is described via an Arrhenius type behavior given by:

$$f_{max}(T) = f_0 \exp(-E_A / k_B T) \tag{2}$$

where f_{max} is the loss peak frequency, f_0 is pre-exponential factor, E_A is the activation energy of the process and k_B the Boltzmann constant. The dependence of α-relaxation's loss peak position on temperature follows the Vogel- Fulcher- Tammann- Hesse (VFTH) relation:

$$f_{max}(T) = f_0 \exp(-B / (T - T_V)) \tag{3}$$

where f_0 is a pre-exponential factor, B is a parameter being a measure of the activation energy of the system and T_V is the Vogel temperature or ideal glass transition temperature, which has been found to lie between 30 and 70 K below experimental value of T_g.

The variation of the AC conductivity and the first derivative of AC conductivity as function of temperature at 0.1 Hz is depicted in Fig. 7a and 7b , respectively. The dependence of conductivity on temperature, at constant frequency, in a dielectric system is expressed by Eq. (2):

$$\sigma(T) = \sigma_0 \exp(-E_A / k_B T) \tag{4}$$

where σ_0 is pre-exponential factor, E_A is the activation energy and k_B the Boltzmann constant. Bearing in mind Eq. (2) it is obvious that conductivity increases with temperature and the derivative $d\sigma/dT$ is positive. However, in composite dielectrics the sign of temperature coefficient of conductivity changes. The modification, at constant frequency, from positive to negative values and vice versa, is considered as a functional behavior of the composite material and it has been referred as a touchstone for the development of smart systems [14]. The alteration of the temperature coefficient of conductivity induces functionality of composites and increases their technological impact.

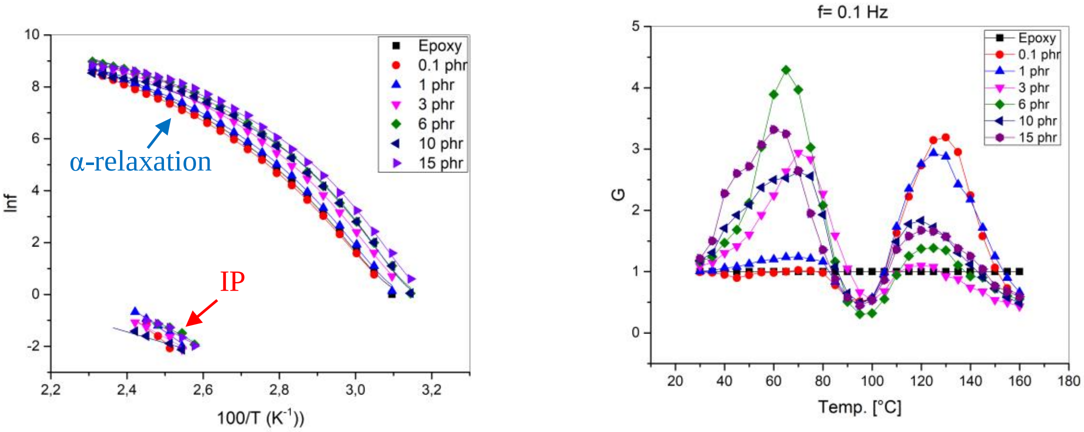

Figure 6. Loss peak potision as a function of frequency and temperature for the α- and β- relaxation mechanisms (left), variation of G as a function of temperature at 0. Hz for specimens (right).

The percentage of stored energy in the composite material relative to the neat epoxy resin specimen has been calculated via the Dielectric renforcing Function (DRF), defined via Eq. (5) and presented in Fig. 7b. :

$$G = \varepsilon_{composite} / \varepsilon_{resin} \tag{5}$$

In Fig. 7b two groups of peaks are clearly formed. The first one indicates the α-relaxation process, associated with the transition from the glass to the rubber phase of the polymer matrix. In addition, on the left side of this peak a "shoulder" appears at about 40 °C, this should probable be attributed to the ferroelectric to the paraelectric phase transition of barium zirconate and indcicates the location of the Curie temperature. The second group of peaks is due to the concentration of agile loads at the interface of the system. The interfaces of the system are between the polymer matrix and the ceramic inclusions but also between filler's grains and are related to the polycrystallinity of $BaZrO_3$.

The presence of the ferroelectric to paraelectric transition, in the vicinity of 40°C, is further supported by the plots of Fig. 8. In Figs. 8a and 8b the formation of intense peaks in permittivity's spectra versus temperature, at two different frequencies, for the barium zirconate nanoparticles is evident. These peaks indicate the characteristic Curie temperature of $BaZrO_3$. The structural transition of $BaZrO_3$ nanoparticles from a polar to a non-polar state and the consequent variation of dielectric permittivity induces an additional term of functionality in $BaZrO_3$/epoxy nanocomposites.

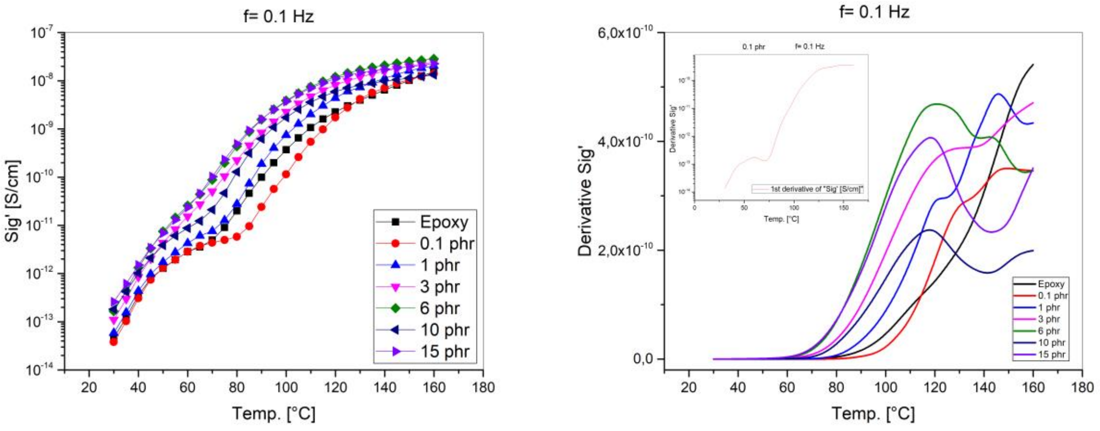

Figure 7. DC conductivity versus temperature at 0.1 Hz for all nanocomposites (left), first derivative of DC conductivity verscus temperature for all nanocomposites at 0.1 Hz (right).

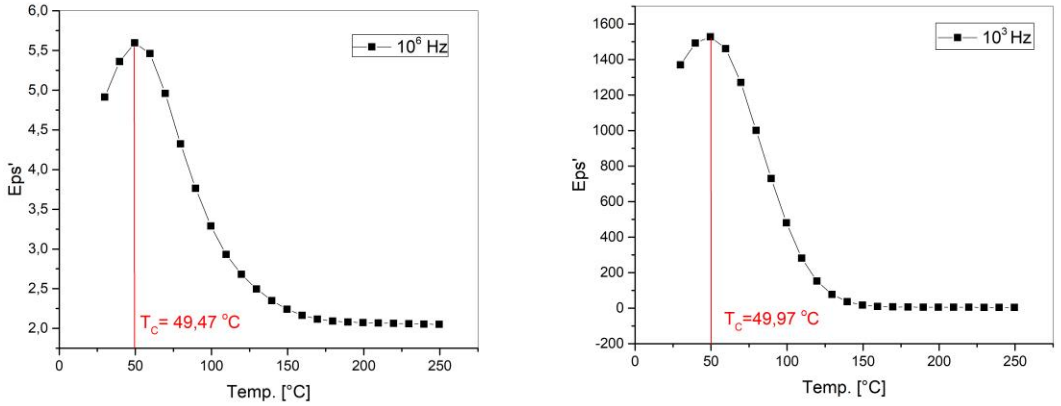

Figure 8. . Real part of dielectric permittivity versus temperature at 10^6 Hz (left) and 10^3 Hz (right) for the $BaZrO_3$ nanoparticles.

3. Conclusions

A series of nanocomposites consisting of epoxy resin and barium zirconate nanoparticles were fabricated in a wide range of loadings and then characterized via broadband dielectric spectroscopy. Ceramic nanoinclusions affect the overall behavior of the composites. The incorporation of the $BaZrO_3$ nanoparticles enhances significantly the dielectric properties of the examined system and induces to them functional behavior. Three relaxation mechanisms were observed in the spectra of all complex systems and were attributed to: (i) Maxwell-Wagner-Sillars effect, recorded at low frequencies and high temperatures, (ii) to α-relaxation observed at intermediate frequencies and ascribed to the glass to rubber transition of the polymer matrix, and (iii) to β-relaxation appeared in the high frequency region due to the re-orientation of small polar groups of the polymer chain. It was also observed that barium zirconate exhibits an unusual dielectric behavior, probably because of its antiferroelectric character. The interactions between the matrix and the nanoinclusions were studied indirectly via the dynamics of relaxations. Finally, the functional behavior of the composite system was investigated via the variation of the temperature coefficient of conductivity, the dielectric reinforcing function and the ferroelectric to paraelectric transition of the $BaZrO_3$ nanoparticles.

References

[1] L.S. Schadler, L.C. Brinson, and W.G. Sawyer, Polymer nanocomposite: a small part of the story, *The Journal of The Minerals, Metals & Materials Society* (3) 53:60,2007.

[2] P. Barber, et al., Polymer composite and nanocomposite dielectric materials for pulse power energy storage, *Materials* 2 (4):1697- 1733, 2009.

[3] T. Hanemann, and D.V. Szabó, Polymer- nanoparticlecomposites: from synthesis to modern applications, *Materials* 3 (6):3468- 3517, 2010.

[4] A.C. Patsidis, K. Kalaitzidou, and G.C. Psarras, Dielectric response, functionality and energy storage in epoxy nanocomposites: barium titanate vs exfoliated graphite nanoplatelets, *Materials Chemistry and Physics*, 798-805, 2012.

[5] A.C. Patsidis., and G.C. Psarras., Structural transition, dielectric properties and functionality in epoxy resin-barium titanate nanocomposites, *Smart Materials and Structures*, (22):115006, 2013.

[6] S. Sarangi, T. Badapanda, B. Behera, and S. Anwar, Frequency and temperature dependence dielectric behavior of barium zirconate titanate nanocrystalline powder obtained by mechanochemical synthesis, *Journal of Materials Science*, 24:4033-4042, 2013.

[7] B.M. Jadwiga, K. Haberko, and M.M. Bucko, Barium zirconate ceramic powder synthesis by the coprecipitation–calcination technique , *Materials Letters*, 56:273- 278 2002.

[8] C. Kittel, *Theory of antiferroelectric crystals*, University of California, Department of Physics, California, Berkley, 1951.

[9] D. Viehland, Transmission electron microscopy study of high- Zr- content lead zirconate titanate, Physical Review B, 52:778 1995.

[10] K.C. Kao, *Dielectric Phenomena in Solids*, Elsevier 1st Edition, 2004.

[11] G. Shirane, E. Sawaguchi, and Y. Takagi, Dielectric properties of lead zirconate, Tokyo Institute of Technology, Oh- okayama, Japan, Tokyo, 1951.

[12] O. Vryonis, D.L. Anastassopoulos, A.A. Vradis, and G.C. Psarras, Dielectric response and molecular dynamics in epoxy-BaSrTiO3 nanocomposites: Effect of nanofiller loading, *Polymer*, 95:82-90, 2016.

[13] A. Sanida, S.G. Stavropoulos, Th. Speliotis, and G.C. Psarras, Development, characterization, energy storage and interface dielectric properties in $SrFe_{12}O_{19}$ / epoxy nanocomposites, *Polymer*, 120:73-81, 2017.

[14] F. El-Tantawy, K.M. Abdel-Kader, F. Kaneko, and Y.K. Sung, Physical properties of CdS-poly (vinyl alcohol) nanoconducting composite synthesized by organosol techniques and novel application potential, *European Polymer Journal*, 40:2, 2004.